Organic & Biomolecular Chemistry

ROYAL SOCIETY OF CHEMISTRY

PAPER

View Article Online
View Journal | View Issue

Check for updates

Cite this: *Org. Biomol. Chem.*, 2021, **19**, 4904

Direct monitoring of biocatalytic deacetylation of amino acid substrates by ^{1}H NMR reveals fine details of substrate specificity†

Silvia De Cesare,[a] Catherine A. McKenna,[a] Nicholas Mulholland,[b] Lorna Murray,[a] Juraj Bella[a] and Dominic J. Campopiano *[a]

Received 22nd January 2021,
Accepted 30th April 2021

DOI: 10.1039/d1ob00122a

rsc.li/obc

Amino acids are key synthetic building blocks that can be prepared in an enantiopure form by biocatalytic methods. We show that the L-selective ornithine deacetylase ArgE catalyses hydrolysis of a wide-range of *N*-acyl-amino acid substrates. This activity was revealed by ^{1}H NMR spectroscopy that monitored the appearance of the well resolved signal of the acetate product. Furthermore, the assay was used to probe the subtle structural selectivity of the biocatalyst using a substrate that could adopt different rotameric conformations.

Open Access Article. Published on 03 May 2021. Downloaded on 5/4/2026 1:46:34 AM.
This article is licensed under a Creative Commons Attribution 3.0 Unported Licence.

Introduction

Reaction monitoring remains a pillar of biocatalysis. It has been employed in the study of the activity, selectivity and substrate scope of wild type enzymes and it is a fundamental platform upon which directed evolution can be applied to engineer novel, more efficient biocatalysts.[1–4] Therefore, the development of robust and reproducible high-throughput (HTP) assays is necessary to achieve fast and reliable measurement of enzymatic activity, kinetic parameters and reaction conversions.[5]

Hydrolases form a well-characterised class of stereoselective biocatalysts, usually employed to develop kinetic resolution (KR), dynamic kinetic resolution (DKR) or de-symmetrisation processes for the isolation of small, enantiopure molecules.[6] Aminoacylases or acylases (EC 3.5.1.14) are important members of this family of enzymes; they specifically catalyse the hydrolysis of the amide bonds of canonical *N*-acetylated amino acids (*N*-Ac-AAs) or derivatives, releasing the free amino acid along with acetate into solution (Scheme 1). Given the high stereoselectivity of these class of enzymes, they are usually employed in the resolution of optically active products from racemic starting materials[7] and to synthesise a range of amides including the penicillin-derived antibiotics.[8] They can be readily combined with *N*-acetyl amino acid racemases (NAAARs or NSARs) to achieve a DKR that can convert racemic *N*-acetylated amino acids into enantiopure products.[9,10] Moreover, some acylases have also been shown to act "in reverse" to catalyse the formation of amides from amino sugars, amino acids and various carboxylic acids.[11,12]

A classic approach to calculate the conversions of these biotransformations is *via* chiral HPLC analysis.[13,14] However, this approach can only be employed when UV-active substrates (*e.g.* aromatic, heterocyclic) are used. Alternative HPLC assays monitor the kinetics of the hydrolytic reaction by observing the disappearance of the *N*-acylated starting material.[15–17] However, given the weak absorbance of the amide bond in the UV region (214 nm, ε = 103 M^{-1} cm^{-1}),[15] the sensitivity of this analysis is quite poor. To overcome this limitation, various colorimetric and fluorometric assays use two main strategies to monitor biocatalysed deacetylation reactions.

The first strategy consists of exploiting a HTP continuous enzymatic assay.[5] For example, three enzymes, an acetate kinase (AK), a pyruvate kinase (PK) and a D-lactate dehydrogenase (LDH) are coupled together in the presence of ATP and phosphoenolpyruvate (PEP) to measure the free acetate formed by linking it directly to the oxidation of NADH to NAD^+ (Scheme S1A†).[18] Similarly, the formation of L-glutamate (L-Glu) can be easily monitored using an NAD^+-dependant L-Glu dehydrogenase (GDH) that catalyses the oxidative deamination of L-Glu to α-ketoglutarate.[19] Sánchez Carrón *et al.*,[20] recently reported a HTP colorimetric assay that detects free

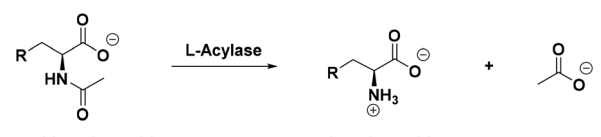

Scheme 1 Synthesis of enantiopure D- or L-amino acids *via* hydrolysis of *N*-acetylated substrates using a stereoselective D- or L-acylase biocatalyst.

[a]*School of Chemistry, University of Edinburgh, David Brewster Road, King's Buildings, Edinburgh, EH9 3FJ, UK. E-mail: Dominic.Campopiano@ed.ac.uk*
[b]*Syngenta, Jealott's Hill, Warfield, Bracknell RG42 6EY, UK*

†Electronic supplementary information (ESI) available. See DOI: 10.1039/d1ob00122a

This journal is © The Royal Society of Chemistry 2021

Open Access Article. Published on 03 May 2021. Downloaded on 5/4/2026 1:46:34 AM.
This article is licensed under a Creative Commons Attribution 3.0 Unported Licence.

amino acids by coupling their production with an FAD-dependant L-amino acid oxidase (L-AAO) and a horseradish peroxidase (HRP) (Scheme S1B†). The resulting H_2O_2 can be linked to the oxidation of *o*-dianisidine at 436 nm (ε = 5700 M^{-1} cm^{-1}) or a similar colorimetric reporter. Although these HTP continuous assays are useful when measuring biocatalyst activity and kinetics, they are not suitable for quantitative analysis as the formation of the product is monitored indirectly *via* a cascade of reactions with a limited linear range.

A second popular strategy often employed for the analysis of free amino acids is the use of derivatization reagents to produce a product with either a strong absorbance or fluorescence in the UV-Vis region. These derivatives are easily detected *via* HPLC or LC-MS analysis. Such reagents include: ninhydrin,[21] *o*-phthalaldehyde (OPA),[22,23] Marfey's reagent (MR)[24] and 4-chloro-7-nitrobenzo-2-oxa-1,3-diazole (NBD).[25] Use of MR also allows for the determination of the enantiomeric excess (% *ee*) of the desired reaction product, since it forms two easily separated diastereoisomers (Scheme S1C†). Amino acids can also be derivatised using various agents, such as alcohols or chloroformates to obtain a volatile product that is readily analysed by GC.[26–29] Unfortunately, all derivatization reactions suffer from a lack of reproducibility, given the possible formation of side-products in the assay mixture. Recently, various LC-MS protocols for the quantitation of free amino acids and MR derivatives in solution have also been developed.[30–32]

Alongside these methods, an ideal candidate for biocatalyst reaction monitoring is ^{1}H NMR spectroscopy. This technique allows the easy calculation of reaction conversions using a relative quantitation method, or the determination of the absolute concentration of starting material and product present in the sample when an appropriate internal standard is employed in a quantitative NMR (qNMR) experiment.[33] Given the various advantages of ^{1}H NMR spectroscopy, such as the easy analysis set-up, short measurement time, direct structural information, high accuracy and its non-destructive nature, this technique had already been applied for the quantitative analysis of active ingredients (AI), natural products and complex biological mixtures.[33,34] Furthermore, ^{1}H NMR spectroscopy has been used to measure biocatalysed reactions; examples include lipase-catalysed acylations[35] and monophosphates ring opening reactions,[36] determination of the % *ee* of hydrolytic KRs,[37,38] and to characterise complex carbohydrate derivatives.[39,40] Here we report the development, optimization and application of a novel ^{1}H NMR assay to monitor amide hydrolysis catalysed by a highly active deacetylase (Scheme S1D†). This was achieved by direct observation (both time dependent and end-point) of the sharp, well-resolved singlet peak associated with the methyl group of the acetate product. Furthermore, we show the wide utility and applicability of this assay, by applying an optimised ^{1}H NMR protocol to determine the % conversion for a series of *N*-acetylated, non-canonical amino acids (NCAAs). Finally, we provide insight into the subtle biocatalyst substrate preference of *N*-acyl amide rotamer conformations.

Results and discussion

^{1}H NMR assay proof of concept

Our target biocatalyst for proof-of-concept studies is the *Escherichia coli N*-acetyl ornithine (*N*-Ac-Orn) deacetylase (ArgE, Uniprot code: P23908, Fig. 1A) which is a di-metal (*e.g.* Zn^{2+}) dependant L-selective acylase with a broad substrate scope.[15,16] ^{1}H NMR is ideal for monitoring deacetylations as the ^{1}H NMR spectrum of an *N*-acetylated amino acid has at least two very distinctive signals, which undergo a shift during hydrolysis (Fig. 1B and C). Catalytic cleavage of the amide bond results in the C-α-proton shifting from 4–5 ppm to 3–4 ppm, while the CH_3 group singlet shifts from the amide substrate at 2.1–1.9 ppm to the acetate product at 1.9–1.8 ppm. By comparing the ratios integrals of these signals, it is possible to calculate the relative conversions of the biocatalysed reaction.[33]

A biotransformation (Fig. 1A) was set up using the natural substrate of the ArgE deacetylase, *N*-Ac-L-Orn (**1a**). Recombinant *E. coli* ArgE was expressed, purified and characterised as reported in ESI (see ESI, Fig. S1 and S2†). The substrate *N*-Ac-L-Orn, **1a** (20 mM) was incubated with ArgE and $CoCl_2$ at 40 °C for 24 h in a final volume of 500 μL. $CoCl_2$ was added to the reaction mixture, since it has been reported that Co(II) increases the activity of ArgE approximately 2-fold.[16]

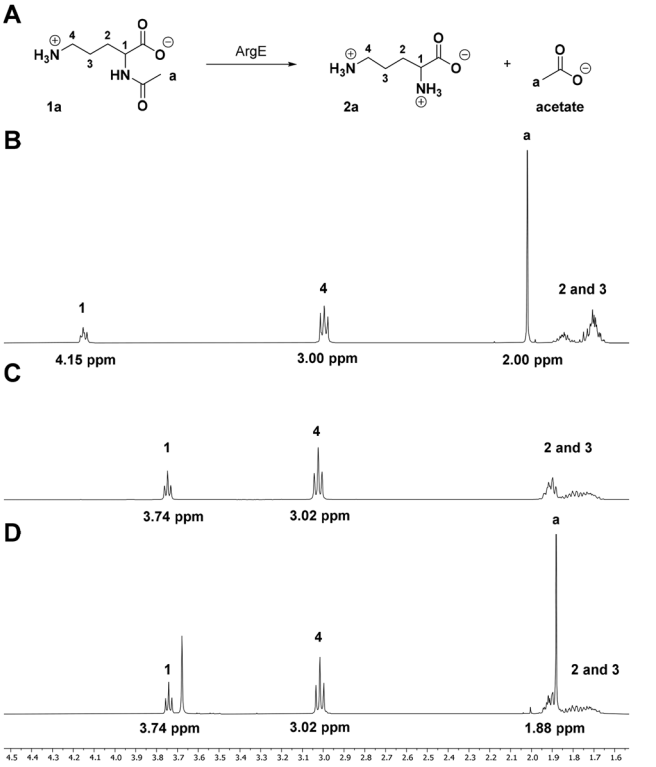

Fig. 1 ^{1}H NMR assay proof of concept. (A) Scheme for the ArgE-catalysed deacetylation of *N*-Ac-L-Orn (**1a**) with ^{1}H NMR spectra with annotated signals. (B) *N*-Ac-L-Orn (**1a**) substrate standard. (C) L-Orn (**2a**) product standard. (D) ArgE biotransformation reaction shows complete conversion of **1a** to **2a** during 24 h at pH 8.0 (the signal at 3.68 ppm is due to the TRIS buffer used during *E. coli* ArgE purification).

Open Access Article. Published on 03 May 2021. Downloaded on 5/4/2026 1:46:34 AM.
This article is licensed under a Creative Commons Attribution 3.0 Unported Licence.

Once L-ornithine (**2a**) formation was confirmed by LC-TOF MS analysis, the biotransformation was quenched by addition of HCl_{conc} to precipitate the enzyme. 100 μL of D_2O was mixed in an NMR tube with 400 μL of the crude reaction mixture and the ^1H NMR spectrum of the sample was recorded on a Bruker AVA500 (500 MHz) NMR. To achieve a higher signal to noise ratio (S/N), a solvent signal suppression experiment was employed. For reference, an NMR spectrum of a standard samples of substrate **1a** and product **2a** were also recorded. By comparing the spectra of standards **1a**, **2a** (Fig. 1B and C) with the reaction mixture (Fig. 1D) it was possible to conclude that the reaction went to completion, following 24 h incubation at 40 °C. This was confirmed by the disappearance of the signals from the C-α proton (multiplet at 4.15 ppm) and the CH_3 from the amide (2.00 ppm) (Fig. 1D). This was also accompanied by the clear CH_3 signal observed for the acetate product at 1.88 ppm (Fig. 1D). It is worth noting that depending on the nature of the substrate side chain, the C-α proton signal of *N*-acetylated amino acids (4–5 ppm region) could fall close to or overlap with the residual peak of water (4.79 ppm). This superimposition can alter the intensity of this signal during the solvent suppression experiment, rendering peak integration inaccurate. However, the acetate singlets of the amide substrate fall in a low-field region of the spectrum (2.1–1.7 ppm), far away from the solvent residual peak, thus, it can be integrated with high accuracy to give a good estimate of the reaction conversion. Furthermore, this signal is generated by three equivalent protons, which should deliver a better S/N ratio and higher assay sensitivity; indeed, sodium acetate is a common internal standard used in qNMR experiments for the determination of the concentrations of the species present in the sample.[32]

Encouraged by the success of our first analysis, we set up a screen of biotransformations following the same reaction protocol, to prove the wide applicability of this assay in the study of enzymatic deacetylations. A panel of nineteen *N*-acetylated L-proteinogenic amino acids (with the exception of *N*-acetyl serine, available only as a racemate) was tested as ArgE substrates (Scheme S2†). All reaction conversions were calculated by comparing the intensity of the methyl signal of the *N*-bound amide substrate and free acetate product (apart from the *N*-Ac-Gln substrate where we used the signals from the C-α-proton, see ESI†). Amino acid product formation was also confirmed by detection *via* LC-MS analysis to back up the ^1H NMR data. The screening results, reported in Table S1,† are in broad agreement with the data reported in literature which used the less sensitive UV-Vis amide bond assay (λ_{max} = 214 nm) to determine the kinetic parameters of ArgE.[14] We found that ArgE displayed a preference for aliphatic and positively charged substrates, whereas acidic (glutamic and aspartic acid) and aromatic (phenylalanine (<2.0% conversion), tyrosine and tryptophan) *N*-acylated amino acids are not hydrolysed by this L-acylase. In addition, our assay was able to identify some novel substrates, such as *N*-Ac-L-valine, arginine, histidine and proline. This data shows how ^1H NMR spectroscopy can be exploited to obtain reliable assays for these amide substrates with higher sensitivity compared to classic spectrophotometric analysis.

Reaction monitoring

Thus far, we have simply employed ^1H NMR spectroscopy to calculate the reaction conversion in an end-point type assay, after prolonged incubation (24 h). However, NMR has been successfully employed to run kinetic experiments to directly monitor various reactions over time.[41–43] Similarly, we employed this technique to follow the progress of the ArgE-catalysed deacetylation reaction. To run these real-time, reaction monitoring experiments *N*-Ac-L-Val (Fig. 2A) was selected as the substrate since this *N*-acetylated amino acid has two signals that fall at low field in the ^1H NMR spectrum. These can be employed to follow the biotransformation progress. The ^1H NMR spectrum was recorded for both the *N*-acyl-L-Val substrate and L-Val reaction product to use as reference (Fig. S3†). We observed both the *N*-acyl singlet (***N*-Ac** at 2.16 ppm) and the signals generated from the two $-CH_3$ groups of the isopropyl side-chain (iPr, $\boldsymbol{\beta_R}$ at 0.98 pm) for *N*-Ac-L-Val.

Two identical reactions were set up in NMR tubes and incubated at 25 °C and 40 °C respectively. A ^1H NMR spectrum was recorded on a Bruker AVA 400 (400 MHz) NMR every 10 min for 2.5 h (Fig. 2B); the first time-point measurement was taken 15 min after the addition of ArgE to the reaction mixture. This lag phase was necessary to set up the experiment and to give enough time for the NMR probe to reach the desired tempera-

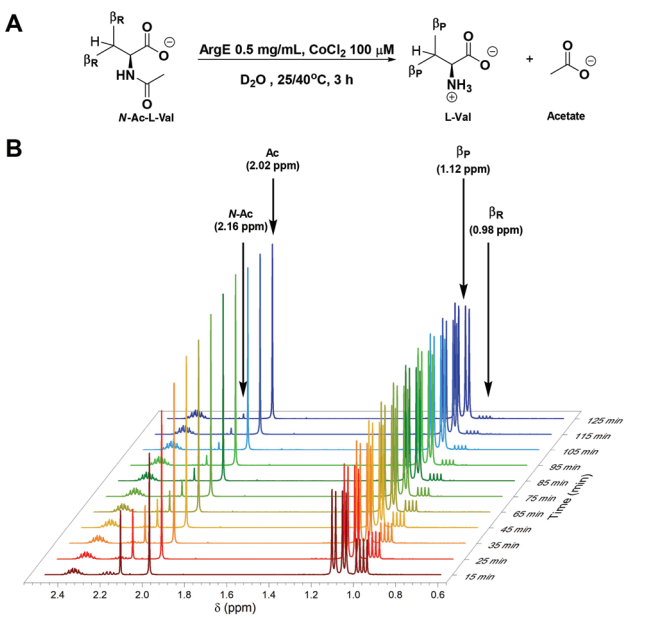

Fig. 2 Direct time-dependant monitoring of the biocatalytic *N*-Ac-L-Val deacetylation by ^1H NMR spectroscopy. (A) Reaction scheme of the ArgE-catalysed *N*-Ac-L-Val hydrolysis. The iPr groups of the substrate ($\boldsymbol{\beta_R}$) and product ($\boldsymbol{\beta_P}$) are labelled. (B) Superimposition of ^1H NMR spectra of the *N*-Ac-L-Val hydrolysis at 40 °C, pH 8.0 during incubation from 15 (dark red) to 125 min (dark blue). The signals for the substrate ($\boldsymbol{\beta_R}$ at 0.98 ppm and ***N*-Ac** at 2.16 ppm) reduce and new signals for the L-Val product ($\boldsymbol{\beta_P}$ 1.12 ppm and **Ac**, 2.02 ppm) appear.

This journal is © The Royal Society of Chemistry 2021

Open Access Article. Published on 03 May 2021. Downloaded on 5/4/2026 1:46:34 AM. This article is licensed under a Creative Commons Attribution 3.0 Unported Licence.

ture. In this initial NMR spectrum, effectively 15 min into the reaction, we observed the appearance of a new signals due to the formation of the acetate (**Ac**, 2.02 ppm) and the L-Val product (β_P at 1.12 pm). Integration of these revealed the reaction progress to be 34%, for the reaction incubated at 25 °C. We then monitored these signals over time (every 10 min) for 3 h. By superimposing the recorded spectra, it was possible to observe the progress of the reaction, with the characteristic signals of the *N*-Ac-L-Val decreasing over time and reached completion at 125 min (Fig. 2B, coloured dark red at 15 min moving to dark blue). At the same time, we observed an increase in the relative abundance of the L-Val product signals (normalised to the acetate CH_3 signal at 2.02 ppm, Fig. 2B). By measuring the integrals of the substrate and product signals for every ^{1}H NMR spectrum recorded, we were able to calculate the percentage conversion of the reaction for each time point at both 25 and 40 °C (Fig. S4A†). We found that 40 °C was the best incubation temperature for ArgE activity, with full conversion (>99%) reached after 2 h incubation, compared with a conversion of 81% for the reaction incubated at room temperature. We also confirmed that the conversion of the substrate follows a linear initial rate after ArgE addition and determined similar specific activities for the reaction monitored by both the ^{1}H NMR and the coupled L-AAO assays (Fig. S4A and S4B†).

N-Acetylated NCAAs library screening

To further emphasise the broad applicability of this ^{1}H NMR assay we prepared and screened a small library of *N*-acetylated, non-canonical L-amino acids (NCAAs). The substrates used in the screen were prepared synthetically from the free amino acid *via* acetylation with an excess of acetic anhydride (see ESI†). The screen of the *N*-Ac-NCAAs substrates was carried out using the standard protocol (see ESI†) and the final conversions, following incubation with ArgE for 24 h, are reported in Table 1.

No activity was detected towards *N*-Ac-*tert* Leu (**1g**) and *N*-Ac-*tert* Bu-Ala (**1h**), probably caused by the large steric bulk of the *tert*-butyl group preventing it being a good ArgE substrate. In contrast, good-to-excellent activity was observed with the eight other substrates tested which displayed a broad range of NCAAs side-chain functionalities. The best substrates were *N*-Ac-Orn (**1a**), *N*-Ac-ω-nitro-Arg (**1e**), *N*-Ac-β-chloro-Ala (**1i**) and also included *N*-Ac-cyclopropyl-Gly (**1f**). The substrate preference defined by the ^{1}H NMR assay can now be compared with that measured using the coupled L-AAO method (Scheme S1B, Table S2†). This revealed a similar substrate profile however the ^{1}H NMR assay has the advantage that it reports directly on ArgE specificity and removes the impact of the substrate preference of the L-AAO coupling enzyme.[20]

Conformational analysis of substrate specificity

Finally, we wanted to further explore the selectivity of ArgE using a substrate that displayed the ability to adopt different conformations in solution. We selected *trans N*-acetyl 2-amino-5-methylhex-3-enoic acid (**1j**) (Fig. 3A, see ESI†) and observed a series of signals in the double bond region of the ^{1}H NMR spectrum of the starting material (Fig. 3B). *N*-Acyl amides are known to form two different conformations (rotamers), due to the restricted rotation around the amide bond. The ratio of minor : major rotamers is dictated by the thermodynamic stability of each conformation.[44,45] We assigned the two doublet of doublets at 5.81 and 5.68 ppm (J = 15.6, 6.5 Hz) as $\mathbf{H_d}$ and $\mathbf{H_b}$ of the minor and major rotamers respectively, with a ratio of 0.7 : 1 of $\mathbf{H_d}$ to $\mathbf{H_b}$ (Fig. 3B). These assignments were confirmed by 2D NMR spectroscopy (see ESI† for NMR characterization). In addition, the multiplet at 5.48–5.41 pm is caused by the overlapping signals of $\mathbf{H_a}$ and $\mathbf{H_c}$ of the major

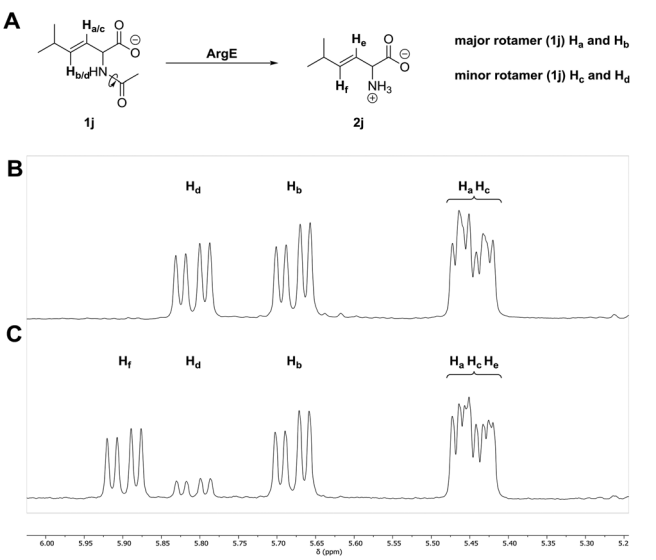

Fig. 3 Determination of the conformational selectivity of *E. coli* ArgE. (A) Reaction scheme for the hydrolysis of the substrate *trans*-2-acetoamido-5-methylhex-3-enoic acid **1j**, present in solution as a mixture of rotamers indicated by the rotation arrow. (B) The double bond region (5–6 ppm) of the ^{1}H NMR spectrum of the two *trans* protons are annotated as follows: $\mathbf{H_a}$ and $\mathbf{H_b}$ for the major rotamer, $\mathbf{H_c}$ and $\mathbf{H_d}$ for the minor rotamer. (C) The same chemical shift region as (B) after incubation of **1j** with ArgE (0.25 mg mL^{-1}) and $CoCl_2$ (100 μM) at 40 °C for 24 h. The ^{1}H NMR integrals for the major rotamer do not change whereas the integrals for the minor rotamer decrease. The appearance of new signals that correspond to the product **2j** are annotated as $\mathbf{H_e}$ and $\mathbf{H_f}$.

Table 1 Conversion percentages determined from the integral of the acetate peak in the ^{1}H NMR spectra (Fig. 1). The *m*/*z* values are from positive ion LC-TOF MS analysis for the ArgE-catalysed production of the corresponding product L-NCAAs (**2a–j**) (N.D. product not detected)

Substrate	R (side-chain)	Conv (%)	m/z $[M + H]^+$
1a	$-CH_2CH_2CH_2NH_2$	>99.0	133
1b	$-CH_2CH_2SOCH_3$	94.3	166
1c	$-CH_2CH_2SO_2CH_3$	76.4	182
1d	$-CH_2SCH_3$	50.7	136
1e	$-CH_2CH_2CH_2NHCNHNHNO_2$	>99.0	220
1f	–Cyclopropyl	60.9	116
1g	$-C(CH_3)_3$	N.D.	N.D.
1h	$-CH_2C(CH_3)_3$	N.D.	N.D.
1i	$-CH_2Cl$	>99.0	124
1j	$-CHCHCH(CH_3)_2$	28.3	144

Open Access Article. Published on 03 May 2021. Downloaded on 5/4/2026 1:46:34 AM.
This article is licensed under a Creative Commons Attribution 3.0 Unported Licence.

and minor rotamers respectively (Fig. 3B). Upon incubation with ArgE we observed the formation of a new signal at 5.90 ppm, $\mathbf{H_f}$, which we assign to the vinyl ^{1}H of **2j**, as well as the reduction of the $\mathbf{H_d}$ signal at 5.81 ppm (Fig. 3C). The other vinyl ^{1}H of the product $\mathbf{H_e}$, appears in the multiplet at 5.48–5.41 ppm (Fig. 3C). Our analysis suggests that ArgE hydrolyses only one of the rotamers (the minor conformation). However, at present we cannot define the absolute conformation of the preferred rotamer (attempts to further define these using variable temperature NMR did not resolve the conformations). This conformational selectivity (atropisomerism) has been observed during the design of *N*-acyl amide inhibitors and it is now incorporated into the design of pharmaceuticals.[46,47] Such detailed substrate analysis is not possible with the HPLC, MS and HTP colorimetric methods.

Conclusions

In conclusion, by employing ^{1}H NMR spectroscopy we were able to develop a quick and efficient assay to monitor biocatalytic deacetylation of various amides. For proof of concept we have used *E. coli N*-Ac-L-ornithine deacetylase (ArgE) and a wide range of canonical *N*-Ac-L-AAs. The comparison of the integrals of the clear signals for the amide starting material and the free acetate product allows for a fast and accurate determination of substrate specificity. The ^{1}H NMR assay can then be employed to run time-dependant experiments to monitor the progress of the hydrolysis over time and determine the % conversion to product. This assay should have broad applicability since hydrolytic enzymes (*e.g.* acylases), are widely used to resolve racemic mixtures and prepare optically active products.[6,7]

Another strength of the ^{1}H NMR assay is its wide applicability for screening substrates, in contrast to other assays which have a restricted scope due to limitations in product detection. We screened ArgE activity towards a large library of substrates (29 *N*-Ac-AAs and *N*-Ac-NCAAs). Furthermore, the ^{1}H NMR assay enabled the conformational selectivity (amide rotamer preference) of the ArgE biocatalyst to be investigated which is beyond the scope of other published methods. Given the simple experimental set-up, fast analysis time and the easy instrument accessibility, this study further supports the potential of ^{1}H NMR based assays in biocatalysis.

The real time monitoring of enzymatic deacetylation reactions could be further improved to achieve accurate time point measurements on a second/minute scale as evidenced by the recent work carried out by Rother and colleagues.[48] Moreover, advances in FlowNMR technology and analysis will accelerate application of these methods.[49] With the optimised ^{1}H NMR assay at hand we can further expand its potential *via* monitoring of acylase-coupled processes, such as biocatalytic DKRs.[13] A combination of improved tools for substrate screening and bioinformatics-driven discovery, coupled with improved methods for directed evolution, will lead to the increased application of biocatalysts for synthesis.[50]

Conflicts of interest

The authors declare no conflict on interests.

Acknowledgements

We thank the Engineering and Physical Sciences Research Council (EPSRC), Syngenta and CRITICAT Centre for Doctoral Training for financial support [Ph.D. studentships to S. D. C. and C. A. McK.; Grant Code: EP/L016419/1]. The NMR facility is supported by EPSRC grant EP/R030065/1. We also thank Prof. Guy Lloyd-Jones and Dr Andrew Hall (University of Edinburgh) for their help and useful comments, as well as Dr Dimitrios Papasotiriou and Dr Peter Howe (Syngenta, Bracknell) for their help in the initial optimization of the ^{1}H NMR and LC-MS experimental protocols. We appreciate the insight provided by Dr Manuela Tosin (University of Warwick) and Dr Amanda Jarvis (University of Edinburgh).

References

1 M. T. Reetz, *Angew. Chem., Int. Ed.*, 2002, **41**, 1335–1338.
2 U. T. Bornscheuer, G. W. Huisman, R. J. Kazlauskas, S. Lutz, J. C. Moore and K. Robins, *Nature*, 2012, **485**, 185–194.
3 F. H. Arnold, *Angew. Chem., Int. Ed.*, 2019, **58**, 14420–14426.
4 U. Markel, K. D. Essani, V. Besirlioglu, J. Schiffels, W. R. Streit, U. Schwaneberg and U. Markel, *Chem. Soc. Rev.*, 2020, **49**, 233–262.
5 H. Bisswanger, *Perspect. Sci.*, 2014, **1**, 41–55.
6 K. Faber, *Biotransformations in Organic Chemistry*, Springer International Publishing, 2011.
7 B. Wang, Y. Liu, D. Zhang, Y. Feng and J. Li, *Tetrahedron: Asymmetry*, 2012, **23**, 1338–1342.
8 K. Buchholz, *Appl. Microbiol. Biotechnol.*, 2016, **100**, 3825–3839.
9 S. Martínez-Rodríguez, P. Soriano-Maldonado and J. Antonio, *Biochim. Biophys. Acta, Proteins Proteomics*, 2020, **1868**, 140377.
10 S. De Cesare and D. J. Campopiano, *Curr. Opin. Biotechnol.*, 2021, **69**, 212–220.
11 M. C. Bourkaib, S. Delaunay, X. Framboisier, C. Humeau, J. Guilbot, C. Bize, E. Illous, I. Chevalot and Y. Guiavarc'h, *Process Biochem.*, 2020, **99**, 307–315.
12 P. Laborda, Y.-M. Lyu, F. Parmeggiani, A.-M. Lu, W.-J. Wang, Y.-Y. Huang, K. Huang, J. Guo, L. Liu, S. L. Flitsch and J. Voglmeir, *Angew. Chem., Int. Ed.*, 2020, **59**, 5308–5311.
13 S. Baxter, S. Royer, G. Grogan, F. Brown, K. E. Holt-Tiffin, I. N. Taylor, I. G. Fotheringham and D. J. Campopiano, *J. Am. Chem. Soc.*, 2012, **134**, 19310–19313.
14 S. L. Lovelock, R. C. Lloyd and N. J. Turner, *Angew. Chem., Int. Ed.*, 2014, **53**, 4652–4656.

 This journal is © The Royal Society of Chemistry 2021

Open Access Article. Published on 03 May 2021. Downloaded on 5/4/2026 1:46:34 AM.
This article is licensed under a Creative Commons Attribution 3.0 Unported Licence.

15 F. Javid-Majd and J. S. Blanchard, *Biochemistry*, 2000, **39**, 1285–1293.
16 W. C. McGregor, S. I. Swierczek, B. Bennett and R. C. Holz, *J. Am. Chem. Soc.*, 2005, **127**, 14100–14107.
17 M. C. Bourkaib, S. Delaunay, X. Framboisier, L. Hôtel, B. Aigle, C. Humeau, Y. Guiavarc'h and I. Chevalot, *Enzyme Microb. Technol.*, 2020, **137**, 109536–109548.
18 S. Mukhopadhyay, M. S. Hasson and D. A. Sanders, *Bioorg. Chem.*, 2009, **36**, 65–69.
19 E. Schmidt, in *Methods of Enzymatic Analysis (Second Edition)*, ed. H. U. Bergmeyer, Academic Press, 2nd edn., 1974, pp. 650–656.
20 G. Sánchez-Carrón, T. Fleming, K. E. Holt-Tiffin and D. J. Campopiano, *Anal. Chem.*, 2015, **87**, 3923–3928.
21 S. Yokoyama and J.-I. Hiramatsu, *J. Biosci. Bioeng.*, 2003, **95**, 204–205.
22 R. Rowlett and J. O. E. Murphy, *Anal. Biochem.*, 1981, **112**, 163–169.
23 S. L. Zandy, J. M. Doherty, N. D. Wibisono and R. A. Gonzales, *J. Chromatogr. B: Anal. Technol. Biomed. Life Sci.*, 2017, **1055–1056**, 1–7.
24 R. Bhushan and H. Bru, *Amino Acids*, 2004, **27**, 231–247.
25 C. Yang, X. Jiang, L. Guo, H. Zhang and M. Liu, *J. Sep. Sci.*, 2007, **30**, 3154–3163.
26 M. T. Reetz, K. M. Kühling, S. Wilensek, H. Husmann, U. W. Häusig and M. Hermes, *Catal. Today*, 2001, **67**, 389–396.
27 H. Zahradníčková, P. Hušek and P. Šimek, *J. Sep. Sci.*, 2009, **32**, 3919–3924.
28 M. Bertrand, A. Chabin, A. Brack and F. Westall, *J. Chromatogr. A*, 2008, **1180**, 131–137.
29 F. Menestrina, J. O. Grisales and C. B. Castells, *Microchem. J.*, 2016, **128**, 267–273.
30 Y. Nakano, Y. Konya, M. Taniguchi and E. Fukusaki, *J. Biosci. Bioeng.*, 2017, **123**, 134–138.
31 A. R. Klein, K. A. B. Hanson and L. Aristilde, *Environ. Chem. Lett.*, 2020, **18**, 229–235.
32 N. J. Ayon, A. D. Sharma and W. G. Gutheil, *J. Am. Soc. Mass Spectrom.*, 2019, **30**, 448–458.
33 S. K. Bharti and R. Roy, *Trends Anal. Chem.*, 2012, **35**, 5–26.
34 A. M. Tomlins, P. J. D. Foxall, M. J. Lynch, J. Parkinson, J. R. Everett and J. K. Nicholson, *Biochim. Biophys. Acta, Gen. Subj.*, 1998, **1379**, 367–380.
35 R. Legner, A. Wirtz and M. Jaeger, *J. Spectrosc.*, 2018, **2018**, 11.
36 M. Akimoto, T. Yu, K. Moleschi, K. Van, G. S. Anand and G. Melacini, *Chem. Commun.*, 2020, **56**, 8091–8094.
37 M. T. Reetz, A. Eipper, P. Tielmann and R. Mynott, *Adv. Synth. Catal.*, 2002, **344**, 1008–1016.
38 K. A. Farley, U. Reilly, D. P. Anderson, B. P. Boscoe, M. W. Bundesmann, D. A. Foley, M. S. Lall, C. Li, M. R. Reese and J. Yan, *Magn. Reson. Chem.*, 2017, **55**, 348–354.
39 S. C. Cosgrove, A. P. Mattey, M. Riese, M. R. Chapman, W. R. Birmingham, A. J. Blacker, N. Kapur, N. J. Turner and S. L. Flitsch, *ACS Catal.*, 2019, **9**, 11658–11662.
40 R. Cairns, A. Gomm, J. Ryan, T. Clarke, E. Kulcinskaja, K. Butler and E. O. Reilly, *ACS Catal.*, 2019, **9**, 1220–1223.
41 S. Meier, *Catal. Commun.*, 2020, **135**, 105894.
42 C. M. L. Lau, G. Jahanmir and Y. Chau, *Acta Biomater.*, 2020, **101**, 219–226.
43 M. J. Smith, C. B. Marshall, F.-X. Theillet, A. Binolfi, P. Selenko and M. Ikura, *Curr. Opin. Struct. Biol.*, 2015, **32**, 39–47.
44 T. Lanyon-Hogg, M. Ritzefeld, N. Masumoto, A. I. Magee, H. S. Rzepa and E. W. Tate, *J. Org. Chem.*, 2015, **80**, 4370–4377.
45 J. S. Laursen, J. Engel-Andreasen, P. Fristrup, P. Harris and C. A. Olsen, *J. Am. Chem. Soc.*, 2013, **135**, 2835–2844.
46 S. R. LaPlante, P. Forgione, C. Boucher, R. Coulombe, J. Gillard, O. Hucke, A. Jakalian, M. Joly, G. Kukolj, C. Lemke, R. McCollum, S. Titolo, P. L. Beaulieu and T. Stammers, *J. Med. Chem.*, 2014, **57**, 1944–1951.
47 J. Clayden, W. J. Moran, P. J. Edwards and S. R. LaPlante, *Angew. Chem., Int. Ed.*, 2009, **48**, 6398–6401.
48 C. Claaßen, K. Mack and D. Rother, *ChemCatChem*, 2020, **12**, 1190–1199.
49 A. M. R. Hall, J. C. Chouler, A. Codina, P. T. Gierth, J. P. Lowe and U. Hintermair, *Catal. Sci. Technol.*, 2016, **6**, 8379–8576.
50 A. Fryszkowska and P. N. Devine, *Curr. Opin. Chem. Biol.*, 2020, **55**, 151–160.